GM-CSF and IL-3 expression increases immune engraftment and tumor infiltration in a humanized patient-derived xenograft model of hepatocellular carcinoma

Kelley Weinfurtner[1,2], David Tischfield[1], Jennifer Crainic[1], Wuyan Li[1], David E. Kaplan[2,3], Terence P.F. Gade[1,3]

[1]Penn Image-Guided Interventions Lab, Department of Radiology, University of Pennsylvania
[2]Department of Gastroenterology and Hepatology, University of Pennsylvania
[3]Corporal Michael J Cresenz VA Medical Center, Philadelphia, PA

Manuscript type: Research
Word count:

Conflicts of interest: The authors have declared that no conflict of interest exists.

Corresponding author: Terence P. F. Gade
Assistant Professor of Radiology and Cancer Biology
University of Pennsylvania Perelman School of Medicine
652 BRB II/III
421 Curie Blvd
Philadelphia, PA 19104-6160
Tel: 215-573-9756
Fax: 215-746-5511
Email: tgade@pennmedicine.upenn.edu

ABSTRACT

Introduction: Immunotherapy has shown promising results in advanced hepatocellular carcinoma (HCC), and relevant model systems are greatly needed to inform treatment paradigms. Transplantation of immunodeficient mice with human hematopoietic cells allows for the development of humanized patient derived xenografts (HIS PDXs); however, these models have limited development of myeloid lineages. We aimed to determine the impact of human GM-CSF and IL-3 expression on tumor immune cell infiltration and tumor growth in a HIS PDX model of HCC.

Materials and Methods: HIS HCC PDXs were generated using NOG (NOD/Shi-*scid*/IL-2Rγ^{null}) and NOG-EXL (huGM-CSF/huIL-3 NOG) mice conditioned with 30mg/kg Busulfan and, 24 hours later, injected with 400,000 CD34+ cells isolated from human fetal livers. HCC tumor tissue from an established PDX line in Matrigel was then implanted subcutaneously (SQ). Immune engraftment was monitored by flow cytometry. Mice were sacrificed when tumors reached 2cm and tumor, blood, liver, and spleen were analyzed by flow cytometry.

Results: HIS NOG-EXL HCC mice demonstrated earlier and persistently increased huCD45+ peripheral blood immune cells compared to HIS NOG HCC mice with 12.1% vs 1.7% at tumor implantation ($p<0.0001$) and 82.1% vs 43.8% at steady state ($p<0.0001$). All major immune cell types were represented in both groups. There was no difference in tumor growth between HIS NOG HCC, HIS NOG-EXL HCC, and control NOG HCC tumors by latency (48.4, 45.5, and 50.5 days, respectively, $p=0.63$) or Gompertzian growth rates (0.32, 0.31, 0.40, respectively, $p=0.68$). At necropsy, HIS NOG-EXL HCC mice had increased huCD45+ immune cells in tumor (27.2% vs 8.6%, $p=0.03$) compared to HIS NOG HCC mice with increased CD4+ regulatory T cells (21.0% vs 11.1%, $p=0.04$), CD4+ T cell PD-1 expression (77.9% vs 49.4%, $p=0.03$), and M2 macrophage phenotype (36.1% vs 17.6%, $p=0.04$).

Conclusions: HIS HCC PDX models demonstrate robust immune infiltration in the peripheral blood, spleen, liver, and SQ HCC tumor, especially in mice expressing human GM-CSF and IL-3. Expression of these human cytokines lead to increased tumor infiltrating immune cells with a higher proportion of regulatory immune cells, suggesting NOG-EXL mice may be a more appropriate model for preclinical trials with immunotherapy.

INTRODUCTION

Hepatocellular carcinoma (HCC) is a leading cause of cancer-related mortality worldwide, as the majority of patients present with unresectable disease at diagnosis and a median survival of less than two years[1,2]. This dismal prognosis underscores the limited therapeutic options for this population. Recently, immunotherapy has emerged as a first line therapy for advanced HCC; however, regimens remain suboptimal due to low response rates and high rates of adverse effects.[3] Biomarkers of response to immunotherapy, such as PD-1/PD-L1 expression and tumor mutational burden, have been valuable in other malignancies, but have not proven predictive of response in HCC.[4] Early data suggests that immune cell phenotyping of HCC tumors may identify patients with greater likelihood of response to immunotherapy[5,6]; however, further understanding of the interaction of the immune microenvironment and immunotherapy outcomes is limited by the paucity of animal models that can recapitulate the heterogeneity of these factors present in human HCC.

Genetically engineered mouse (GEM) models can be highly useful to study the impact of a single or combined genetic alterations on tumor development and biology, but they lack the heterogeneity and complexity of genetic and epigenetic alterations present in human HCC.[7,8] Chemotaxic models allow for tumors to develop in a background of chronic liver disease as they do in patients, leading to greater genetic diversity and increased fidelity to the tumor microenvironment seen in patients, noting that tumorigenesis will be more variable and potentially time consuming. In both models, tumor formation occurs in immunocompetent mice, allowing for investigations into interactions between HCC tumors and the immune system with several important limitations. First, there can be major differences in the druggability of immunotherapy targets between human and murine homologs, and many of the FDA-approved immunotherapies do not bind the equivalent mouse targets.[9] Second, GEM tumors tend to be nonimmunogenic and often require additional strategies to mimic human immunosurveillance and immunotherapy responses.[10,11] Lastly, while the murine immune system has been used

frequently as a proxy for the human immune system, there are notable known and likely unknown differences in both innate and adaptive immunity.[12]

Patient-derived xenograft (PDX) models, in which human tumors are implanted into highly immunodeficient mice, have been shown to be representative of the heterogeneity of human tumors and patient response to therapy, making them important tools for preclinical therapeutic trials.[13,14] HCC PDXs have been described, but have largely been generated from patients with surgically cured, early-stage disease - likely to reflect less aggressive HCC variants that may never require systemic therapies such as immunotherapy. More recently, our lab and others have demonstrated the ability to generate HCC PDXs from biopsy samples, allowing for the development of PDX lines from patients with intermediate and advanced HCC – the patient population that will be considered for immunotherapy.[15.16] However, the lack of immune system in these models limit their utility in modeling interactions with the immune system and response to immunotherapies.

To overcome this limitation, immunodeficient mice can be xenotransplanted with human hematopoietic stem and progenitors cells to generate mice with humanized immune systems (HIS).[17-19] Engrafting human CD34+ cells into Nod-*scid* IL2Rγ^{null} (NSG) or NOD/Shi-*scid*/IL-2Rγ^{null} (NOG) immunodeficient mice results in HIS mice that produce all lineages of hematopoietic cells, including both innate and adaptive immune cells. While myeloid progenitor cells engraft well in the bone marrow, there are low rates of mature myeloid cells in the periphery of these mice, including cells important for HCC-immune interaction such as macrophages, neutrophils, and dendritic cells.[19-20] Further, the only published model of HCC in HIS mice demonstrated that the presence of HCC tumors leads to significant decrease in all human cells in the periphery.[21] The expression of various human cytokines has been shown to alter the proportion and functionality of different immune cell populations. Specifically, the expression of human granulocyte-macrophage colony-stimulating factor (GM-CSF) and interleukin-3 (IL-3) increases not only overall hematopoietic cell engraftment, but also leads to a

3-fold increase in myeloid cells in the periphery.[22-24] Interestingly, expression of these cytokines also leads to increased infiltration of regulatory T cells into all compartments, including tumor microenvironments.[22] We aimed to investigate what impact the expression of these cytokines has on HCC tumor growth and tumor immune infiltration in order to optimize HIS HCC PDX for the studies of the tumor immune microenvironment and response to immunotherapies.

RESULTS

NOG-EXL mice have increased peripheral immune engraftment, especially myeloid lineages

HIS NOG-EXL mice demonstrated earlier and persistently increased huCD45+ peripheral blood immune cells compared to HIS NOG HCC mice with 12.1% vs 1.7% of cells at 4 weeks post-implantation ($p<0.0001$) and 82.1% vs 43.8% of cells at steady state ($p<0.0001$, **Figure 1A**). All major immune cell types were represented in both groups, including B cells, T cells, NK cells, monocytes, dendritic cells, and neutrophils (**Figure 1B, Supp Figure 1A-F**). HIS NOG-EXL mice had a 2.0-fold increase in B cells, 2.7-fold increase in neutrophils, and 5.5-fold increase in monocytes in the peripheral blood compared to NOG mice at 9 weeks post-implantation, though no difference in total number of T cells, NK cells, or dendritic cells (**Figure 1C-H**). Human immune cells were also found in the liver (7.5% vs 3.2% of cells, $p=0.004$) and spleen (90.4% vs 73.2% of cells, $p=0.01$) of both HIS NOG and HIS NOG-EXL mice, respectively (**Figure 1I-J**) with increased total number of all major immune cells except similar number of dendritic cells in HIS NOG-EXL mice compared to HIS NOG mice (**Supp Figure 1G-R)**. As seen in the peripheral blood, HIS NOG-EXL mice also had a proportional increase in monocytes (3.8% vs 0.7% of huCD45+ cells, $p<0.01$) and neutrophils (3.3% vs 1.5% of huCD45+ cells, $p<0.01$) in the liver compared to HIS NOG mice (**Figure 1K-P**). Notably, there was no difference in T cell subtypes (CD4+, CD8+, Th1, Th17, Treg, naïve, effector) or PD-1 expression between the two cohorts in liver, spleen, or peripheral blood (**Supp Figure 2**).

Humanized immune system does not impact PDX tumor growth rates but does decrease orthotopic tumor engraftment

All HCC tumor implanted subcutaneously (SQ) engrafted regardless of mouse background (8/8 for HIS NOG, 5/5 for HIS NOG-EXL); however, orthotopic tumors only engrafted in only 3/8 (37.5%) of HIS NOG mice and 0/4 (0%) HIS NOG-EXL mice compared to 2/3 (66.7%) in NOG control (**Figure 2A**). In the subcutaneous cohort, there was no difference in tumor growth by latency (48.4, 45.5, and 50.5 days, p=0.63) or standardized growth rates (0.32, 0.31, 0.40, p=0.68) in HIS NOG, HIS NOG-EXL, and control NOG HCC, respectively, though there was increased variability in HIS NOG-EXL mice (**Figure 2B-D**). Similarly, for the orthotopic tumors that did grow, there was no difference in latency or standardized growth rates (data not shown).

HIS NOG-EXL mice have increased tumor immune infiltration with a higher proportion of regulatory immune cells

At necropsy, HIS NOG-EXL mice had increased huCD45+ immune cell infiltration into SQ HCC tumors compared to HIS NOG mice as measured by flow cytometry (57.6% vs 22.7% of live cells, p<0.01, **Figure 2E**) and immunohistochemistry (117.3 vs 36.4 cells/HPF, p=0.02, **Figure 2K**). This included increased T cell infiltration in these tumors (flow cytometry: 8.7% vs 2.6% of live cells, p=0.047, **Figure 2F** and IHC: 14.8 vs 3.3 cells/HPF, p=0.02, **Figure 2L**), specifically fewer naïve T cells (7.9% vs 31.7% of T cells, p=0.02, **Figure 2I-J**) with increased total CD4+ cells (6.7% vs 1.6% of live cells, p=0.02), CD4+ regulatory T cells (13.9% vs 7.0% of T cells, p=0.04), and CD4+ T cell PD-1 expression (77.9% vs 33.9% of CD4+ cells, p=0.01, **Figure 2G-I**). HIS NOG-EXL mice also have increased tumor-associated neutrophils (TANs,) and macrophages (TAMs, 112.8 vs 9.4 cells/HPF, p<0.01, **Figure 2M**). Notably, the proportion of regulatory M2 macrophages were also increased (36.1% vs 17.6% of macrophages, p=0.04).

Presence of HCC tumor influences systemic cytokine populations and peripheral immune engraftment

DISCUSSION

MATERIALS AND METHODS

Humanized mice

NOG (NOD.Cg-*Prkdc*^{scid} *Il2rg*^{tm1Sug}) or NOG-EXL [NOD.Cg-*Prkdc*^{scid} *Il2rg*^{tm1Sug} Tg(SV40/HTLV-IL3,CSF2)] mice were obtained from Taconic and human fetal liver-derived CD34+ hematopoietic stem/progenitor cells were obtained from the University of Pennsylvania's Stem Cell Xenograft Core. The mice were conditioned with intravenous (i.v.) injection of 35 mg/kg busulfan and then injected with 400,000 human CD34+ cells by tail vein 24 hours later.

Humanized HCC PDX generation

HCC PDX was generated from percutaneous biopsy of a patient's HCC tumor implanted into NSG mice and serially passaged as previously described.[16] Immune engraftment was confirmed by the presence of human CD45+ cells in the peripheral blood at 4 weeks post-CD34+ cell transplant. HCC PDX tissue was then implanted with Matrigel subcutaneously (SQ) into the flank or orthotopically into the liver of the humanized mice and growth monitored with calipers or ultrasound, respectively. Sham implantations with Matrigel only were also implanted SQ or orthotopically. Mice were sacrificed once the tumor reached 20 mm in any direction or at end of experiment if no tumor growth.

Immune cell analysis by flow cytometry

Immune engraftment was monitored by flow cytometry on peripheral blood samples obtained from retro-orbital collection every 2 weeks. At necropsy, peripheral blood, tumor, liver, and spleen were harvested. Tissue was mechanically dissociated through 70 micron filter and all samples underwent lysis of red blood cells with ACK lysis buffer prior to antibody staining using

the antibodies listed in supplemental table 1. Flow cytometry panels were analyzed using the gating strategies shown in supplemental figure 1.

Immunohistochemistry analysis

At necropsy, portions of tumor, liver, and spleen were fixed in formalin for subsequent paraffin embedding. Tissue was stained using antibodies for total human cells (huCD45***), T cells (huCD3+), cytotoxic T cells (huCD8+), B cells (huCD19+), natural killer cells (huCD56+), and macrophages (huCD68+), as listed in supplemental table 2. Cell per high power field (HPF) were averaged from ***.

Cytokine/chemokine analysis

Plasma was obtained from biweekly peripheral blood samples collected as previously discussed. Cytokine and chemokine concentrations were determined using a custom Luminex assay from Bio-Techne that included beads for CCL2, CCL4, CCL5, CCL20, CXCL1, CXCL5, CXCL10, CXCL13, granzyme A, GM-CSF, IL-2, IL-3, IL-4, IL-5, IL-6, IL-10, IL-12, IL-17/IL-17A, interferon-gamma, and TNF-alpha, as well as the following angiokines – angiopoietin-1, angiopoietin-2, Tie-2, and VEGF.

Statistics

Study approval

All manipulations with mice were approved by Institutional Animal Care and Use Committee at our institution. All animal experimental procedures were conducted in accordance with the approved protocols and Guide for the Care and Use of Laboratory Animals.

Data availability

Individual FCS files for flow analysis and other primary data can be accessed from corresponding author on request.

AUTHOR CONTRIBUTIONS

KW: designed research studies, conducted experiments, analyzed data, wrote the manuscript

DT: carried out experiments, analyzed data, revised manuscript

JC: carried out experiments, revised manuscript

WL: carried out experiments, revised manuscript

DK: designed research studies, revised manuscript

TG: designed research studies, analyzed data, revised manuscript

ACKNOWLEDGEMENTS

Research reported in this publication was supported by Penn Center for Precision Medicine Accelerator Grant and VA CSR&D I01 CX-001933. KW is supported by CTSA KL2 Mentored Career Development Award. The authors would also like to acknowledge the Stem Cell Xenograft Core (RRID: SCR_010035), the Center for Molecular Studies in Digestive and Liver Diseases (P30DK050306), and the Molecular Pathology and Imaging Core (RRID: SCR_022420).

REFERENCES

1. Bray, F. *et al.* Global cancer statistics 2018: GLOBOCAN estimates of incidence and mortality worldwide for 36 cancers in 185 countries. *CA. Cancer J. Clin* 2018; 68: 394–424.
2. Park, J. W. *et al.* Global patterns of hepatocellular carcinoma management from diagnosis to death: The BRIDGE Study. *Liver Int.* 2015;35:2155–2166.
3. Finn, R. S. *et al.* Atezolizumab plus Bevacizumab in Unresectable Hepatocellular Carcinoma. *N. Engl. J. Med.* 2020;382:1894–1905.
4. Pinter, M., Jain, R. K. & Duda, D. G. The Current Landscape of Immune Checkpoint Blockade in Hepatocellular Carcinoma: A Review. *JAMA Oncol.* 2021;7(1):113-123.
5. Sia, D. *et al.* Identification of an Immune-specific Class of Hepatocellular Carcinoma Based on Molecular Features. *Gastro*. 2017;153:812-826.
6. Llovet, J. M., Montal, R., Sia, D. & Finn, R. S. Molecular therapies and precision medicine for hepatocellular carcinoma. *Nat Rev Clin Oncol*. 2018;15:599–616.
7. Brown, Z. J., Heinrich, B., & Greten, T. F. Mouse models of hepatocellular carcinoma: an overview and highlights for immunotherapy research. *Nat Rev Gastro Hep.* 2018;15:536-554.
8. Olson, B., Li, Y., Lin, Y., Liu, E. T., & Patnaik, A. Mouse models for cancer immunotherapy research. *Cancer Discov.* 2018; 1358-1365.
9. Magiera-Mularz, K. et al. Human and mouse PD-L1: similar molecular structure, but different druggability profiles. *iScience*. 2020;24(1):101960.
10. Ruiz de Galarreta, M. et al. B-catenin activation promotes immune escape and resistance to anti-

PD-1 in hepatocellular carcinoma. *Cancer Discov.* 2019;9(8):1125-1141.

11. Wang, J. et al. UV-induced somatic mutations elicit a functional T cell response in the YUMMER1.7 mouse melanoma model. *Pigment Cell Melanoma Res*. 2017;30(4):428-435.

12. Mestas, J. and Hughes, C. C. W. Of mice and not men: differences between mouse and human immunology. *J. Immun*ol. 2004;172:2731-2738.

13. Gao H. et al. High-throughput screening using patient-derived tumor xenografts to predict clinical trial drug response. *Nat Med.* 2015;21:1318–25.

14. Byrne, A. T. et al. Interrogating open issues in cancer precision medicine with patient-derived xenografts. *Nat. Rev. Cancer.* 2017;17(4):254-268.

15. Blumer, T. et al. Hepatocellular Carcinoma Xenografts Established From Needle Biopsies Preserve the Characteristics of the Originating Tumors. *Hepatol. Commun.* 2019;3:971–986.

16. Tischfield, D. et al. Establishment of Hepatocellular Carcinoma Patient-Derived Xenografts from Image-Guided Percutaneous Biopsies. *Sci Rep*. 2019;9:10546.

17. Yahata, T. et al. Functional human T lymphocyte development from cord blood CD34+ cells in nonobese diabetic/Shi-scid, IL-2 receptor null mice. *J. Immunol*. 2002;169:204–209.

18. Shultz L. D. et al. Human lymphoid and myeloid cell development in NOD/LtSz-scid IL2R gamma null mice engrafted with mobilized human hemopoietic stem cells. *J Immunol*. 2005;174:6477–89.

19. Shultz L. D. et al. Humanized mice for immune system investigation: progress, promise and challenges. *Nat Rev Immunol.* 2012;12:786–98.

20. Tanaka, S. et al. Development of mature and functional human myeloid subsets in hematopoietic stem cell-engrafted NOD/SCID/IL2ryKO mice. *J Immunol.* 2012;188(12):6145-6155.

21. Zhao, Y. et al. Development of a new patient-derived xenograft humanised mouse model to study human-specific tumour microenvironment and immunotherapy. *Gut.* 2018;67:1845–1854.

22. Bilerbeck, E. et al. Development of human CD4+FoxP3+ regulatory T cells in human stem cell factor-, granulocyte-macrophage colony-stimulating factor-, and interleukin-3-expressing NOD-SCID IL2R-gamma(null) humanized mice. *Blood*. 2011;117(11):3076-3086.

23. Maser, I. P. et al. The tumor milieu promotes functional human tumor-resident plasmacytoid dendritic cells in humanized mouse models. *Front Immunol.* 2020:11;2082.

24.

15. Zhao, Y. et al. Analysis and Validation of Human Targets and Treatments Using a Hepatocellular Carcinoma Immune Humanized Mouse Model. *Hepatol.* 2021;74:1395-1410.

16. Maser, I. et al. The Tumor Milieu Promotes Functional Human Tumor-Resident Plasmacytoid and Dendritic Cells in Humanized Mouse Models. *Front Immuno.* 2020;11:2082.

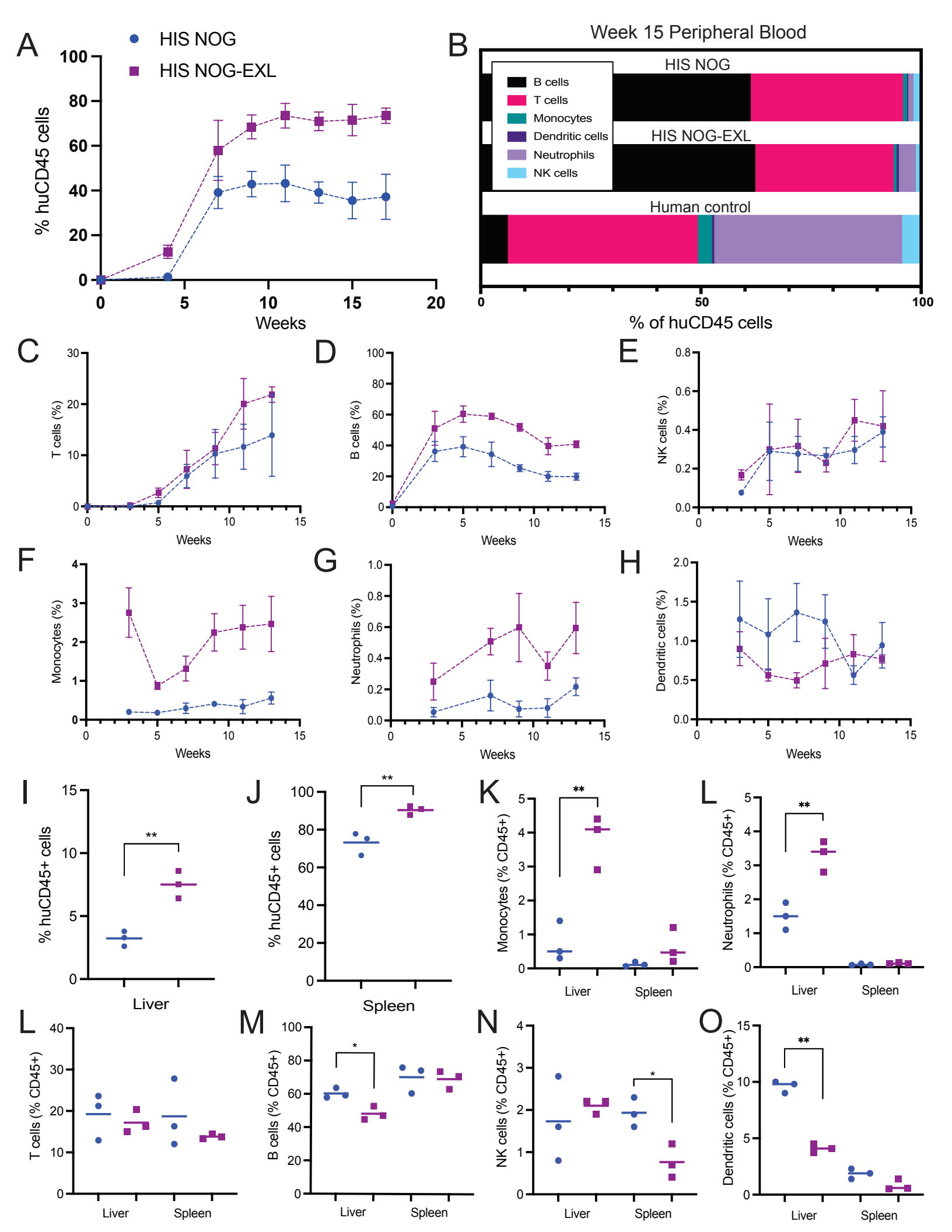
A
HIS NOG
HIS NOG-EXL
% huCD45 cells
Weeks
B
Week 15 Peripheral Blood
HIS NOG
HIS NOG-EXL
Human control
B cells
T cells
Monocytes
Dendritic cells
Neutrophils
NK cells
% of huCD45 cells
C
T cells (%)
Weeks
D
B cells (%)
Weeks
E
NK cells (%)
Weeks
F
Monocytes (%)
Weeks
G
Neutrophils (%)
Weeks
H
Dendritic cells (%)
Weeks
I
% huCD45+ cells
Liver
J
% huCD45+ cells
Spleen
K
Monocytes (% CD45+)
Liver
Spleen
L
Neutrophils (% CD45+)
Liver
Spleen
L
T cells (% CD45+)
Liver
Spleen
M
B cells (% CD45+)
Liver
Spleen
N
NK cells (% CD45+)
Liver
Spleen
O
Dendritic cells (% CD45+)
Liver
Spleen

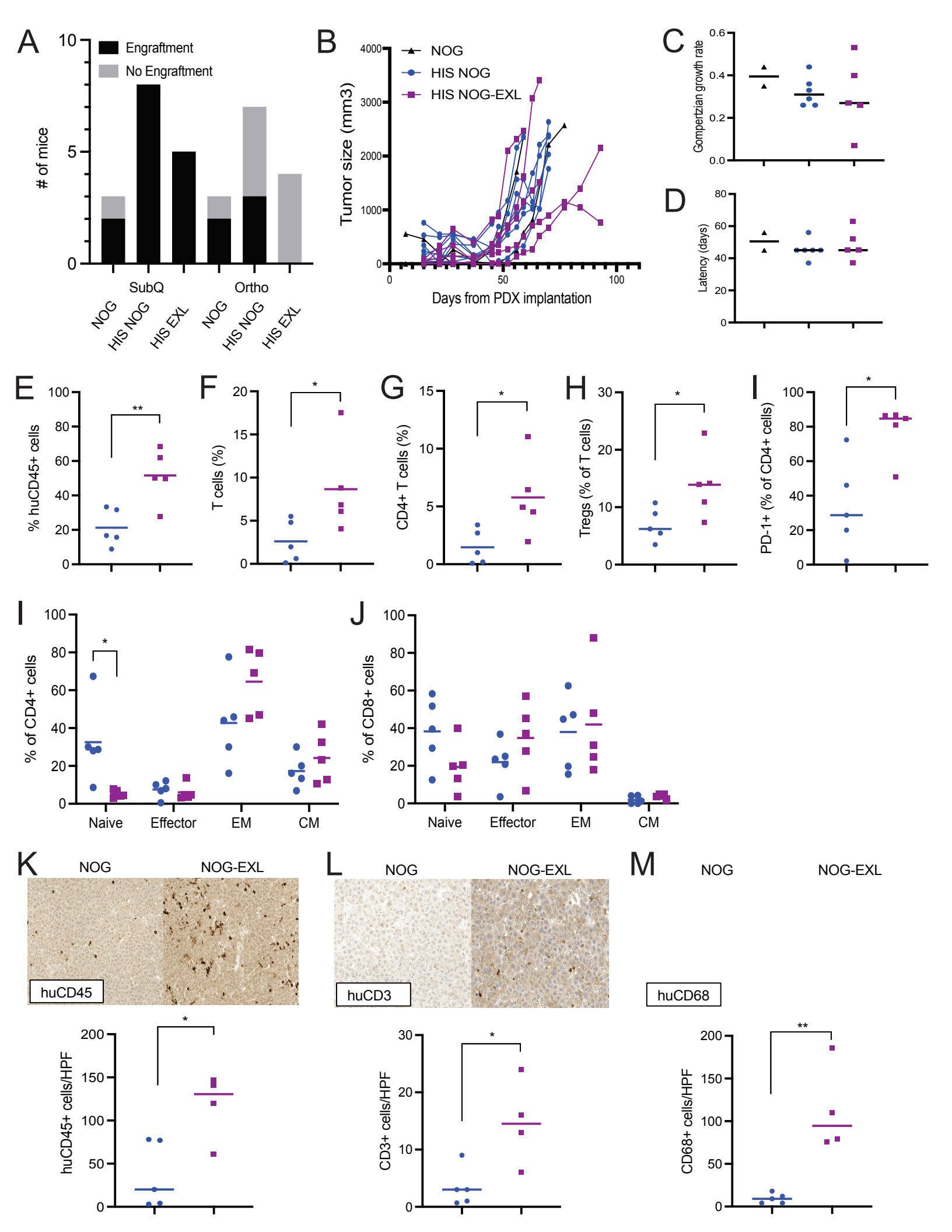
A
Engraftment
No Engraftment
# of mice
SubQ
Ortho
NOG
HIS NOG
HIS EXL
B
NOG
HIS NOG
HIS NOG-EXL
Tumor size (mm3)
Days from PDX implantation
C
Gomperizian growth rate
D
Latency (days)
E
% huCD45+ cells
F
T cells (%)
G
CD4+ T cells (%)
H
Tregs (% of T cells)
I
PD-1+ (% of CD4+ cells)
I
% of CD4+ cells
Naive
Effector
EM
CM
J
% of CD8+ cells
K
NOG
NOG-EXL
huCD45
huCD45+ cells/HPF
L
huCD3
CD3+ cells/HPF
M
huCD68
CD68+ cells/HPF

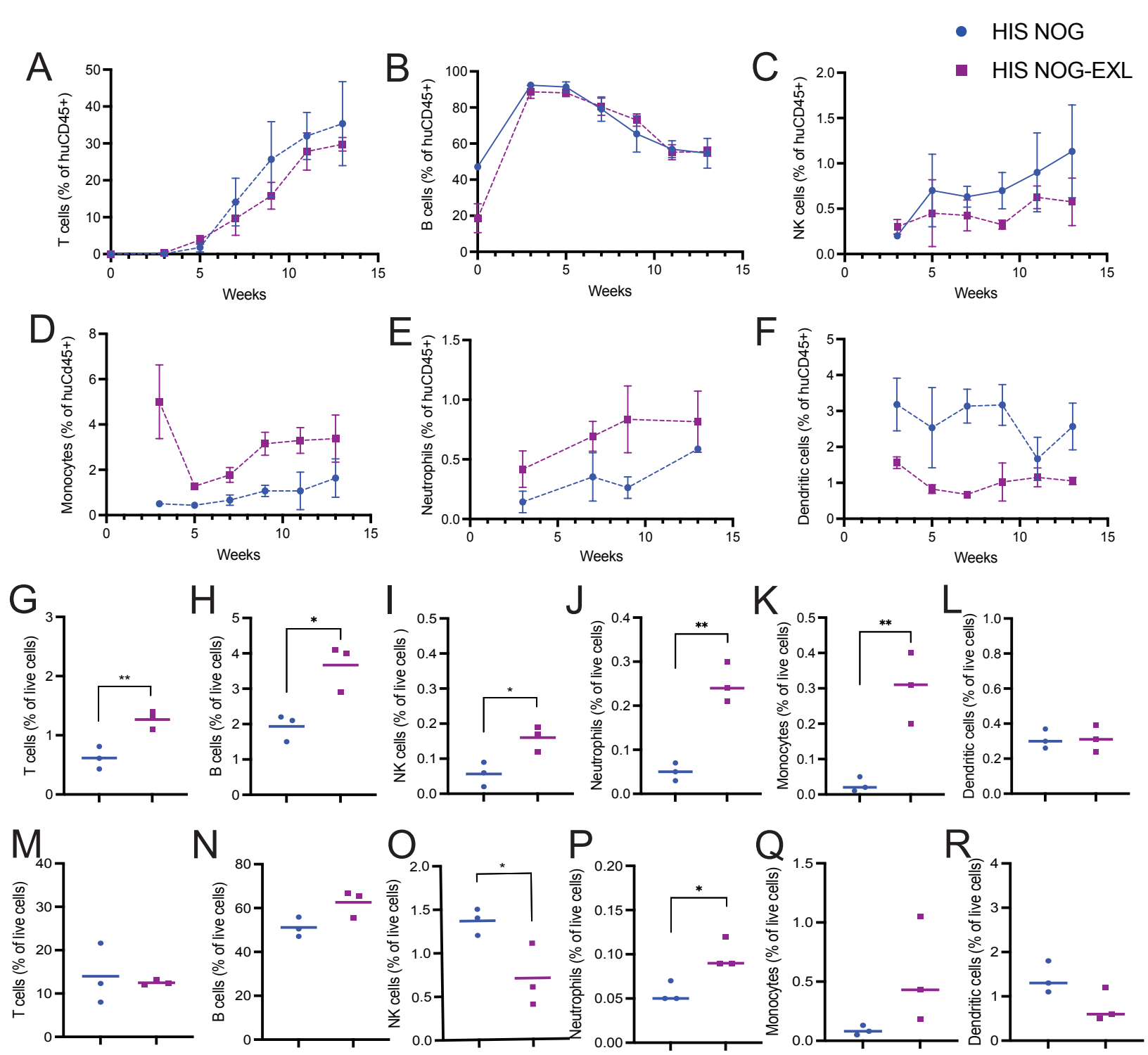
HIS NOG
HIS NOG-EXL
A
T cells (% of huCD45+)
Weeks
B
B cells (% of huCD45+)
Weeks
C
NK cells (% of huCD45+)
Weeks
D
Monocytes (% of huCd45+)
Weeks
E
Neutrophils (% of huCD45+)
Weeks
F
Dendritic cells (% of huCD45+)
Weeks
G
T cells (% of live cells)
H
B cells (% of live cells)
I
NK cells (% of live cells)
J
Neutrophils (% of live cells)
K
Monocytes (% of live cells)
L
Dendritic cells (% of live cells)
M
T cells (% of live cells)
N
B cells (% of live cells)
O
NK cells (% of live cells)
P
Neutrophils (% of live cells)
Q
Monocytes (% of live cells)
R
Dendritic cells (% of live cells)

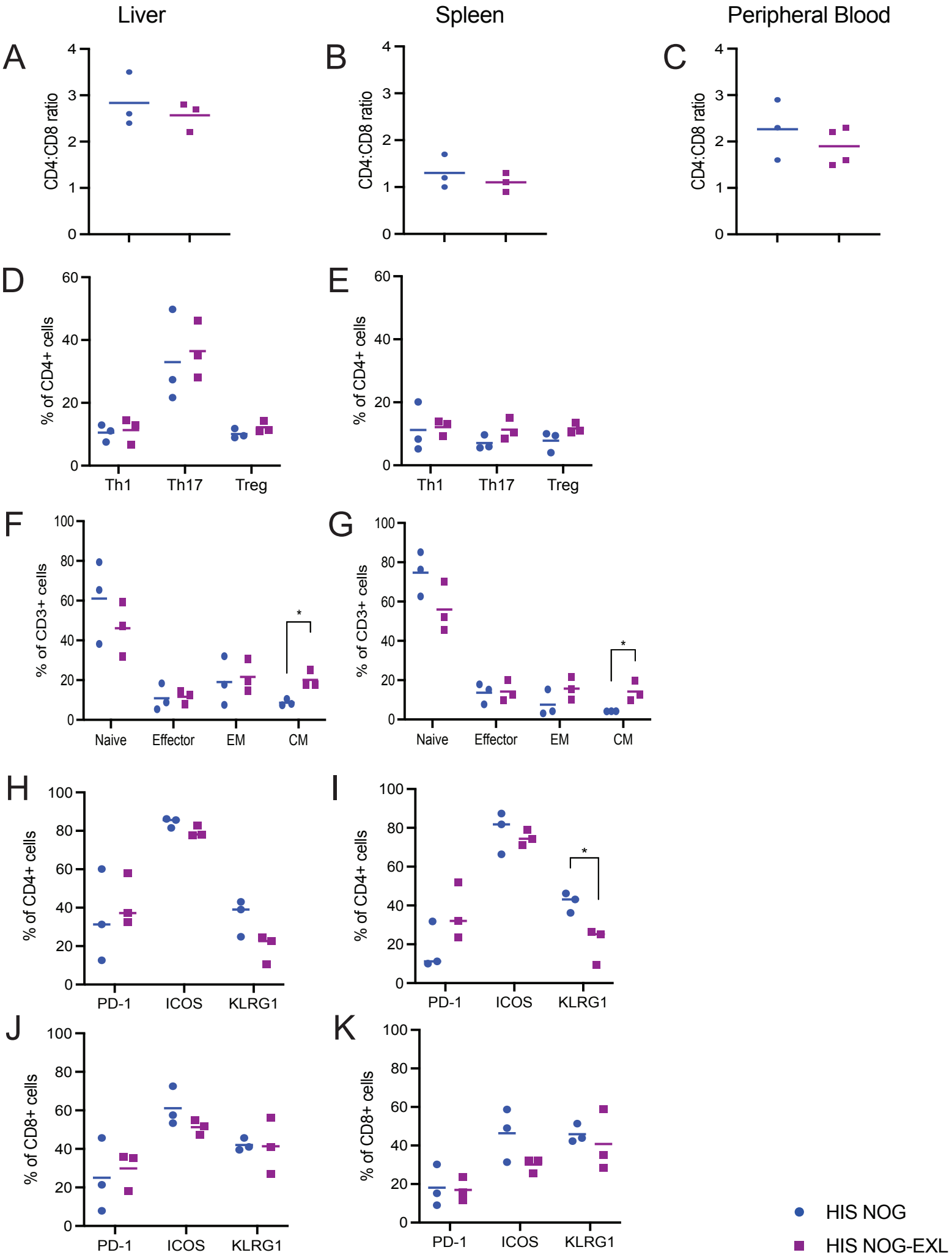
Liver
Spleen
Peripheral Blood
A
B
C
CD4:CD8 ratio
D
E
% of CD4+ cells
Th1
Th17
Treg
F
G
% of CD3+ cells
Naive
Effector
EM
CM
*
H
I
PD-1
ICOS
KLRG1
J
K
% of CD8+ cells
HIS NOG
HIS NOG-EXL